Pergamon

Deep-Sea Research I, Vol. 41, No. 1, pp. 81–100, 1994
Elsevier Science Ltd
Printed in Great Britain
0967–0637/94 $6.00+0.00

The sea surface salinity in the tropical Atlantic between 10°S and 30°N—seasonal and interannual variations (1977–1989)

ALAIN DESSIER* and JEAN RENÉ DONGUY†

(*Received* 14 *April* 1992; *in revised form* 16 *February* 1993; *accepted* 12 *March* 1993)

Abstract—The seasonal and interannual variations of the Sea Surface Salinity (SSS) are analysed in the tropical Atlantic (15°S–30°N, 80°W–15°E) from observations collected by merchant ships between 1977 and 1989 and earlier by ORSTOM research vessels. The harmonic analysis of SSS shows a well defined seasonal cycle both within a 5°N–15°N zonal belt and west of 50°W at higher latitudes. In the eastern Atlantic between 10 and 20°N (along the shipping lanes West Africa–South Africa and West Africa–Brazil), SSS increased from 1977 to 1985, particularly near 10°N. SSS variability is mostly related to the river outflow (Amazon, Orinoco and Congo) west of 40°W and in southern Gulf of Guinea. In the eastern Atlantic, precipitation associated with the ITCZ largely control the SSS seasonal variations.

INTRODUCTION

IN tropical areas, away from the coastal boundaries and shelves, the spatial distribution and temporal variability of the Sea Surface Salinity (SSS) are caused by the evaporation–precipitation balance, advection and mixing. SSS is therefore an index of the intensity and the location of the water exchanges at the air–ocean interface. In the vicinity of the continents, the discharge of rivers drastically changes the SSS, and the spreading of these fresh tongues can be used as tracers of the oceanic circulation.

Earlier studies of SSS by TAYLOR and STEPHENS (1980), LEVITUS (1986, 1989) and NEUMANN *et al.* (1975) have documented seasonal and interannual variations in the Atlantic. An extensive survey of the tropical zone is described in the present publication. After consideration of data and methods, the annual cycle of the SSS in the whole tropical Atlantic is described. We then show that the Western Tropical Atlantic is influenced mainly by the Amazon River while the Eastern Tropical Atlantic is mostly influenced by precipitation. The relation between SSS and the freshwater balance is then considered, and finally some evidence of long-term evolution of the SSS will be presented.

DATA AND METHODS

About 90% of the data outside the Gulf of Guinea have been collected by ships of opportunity. A water sample is gathered at the sea surface, four times a day, using a bucket

*Centre ORSTOM de BREST, B.P. 70, 29280 Plouzane, France.
†ORSTOM and Division of Oceanography, CSIRO, G.P.O. Box 1538, Hobart, Tasmania, Australia.

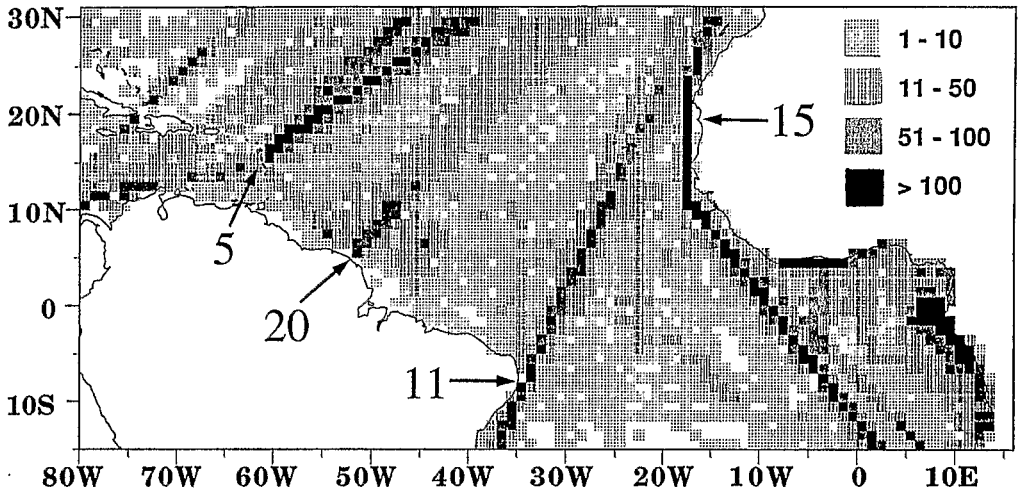

Fig. 1. Density of SSS observations per 1° × 1° square.

and is preserved in a sealed jar; later, salinity is determined by a Guidline Auto Sal 8400A salinometer (DONGUY *et al.*, 1980). This program, following an earlier one (BERRIT, 1961, 1962) started in 1977, totalling more than 57,000 surface salinity observations by December 1989.

Some observations have been compared to nearby surface salinities done with a CTD aboard research vessels for maximum space and time separations of 30 nautical miles and 15 days. The mean difference (0.1 p.s.u.) shows the higher values from the bucket measurements aboard ships of opportunity. DELCROIX and HENIN (1991) have found a comparable mean difference (0.083 p.s.u.). This overestimate of the bucket measurements can have several explanations: salt in the bucket due to the evaporation of the remnants of the previous sample, influence of the ship which, according to its load and its draught may break down the salinity vertical stratification, the imperfect sealing of the jars stored during several weeks.

Although discontinuous time–space sampling may be questionable for describing low frequency variability, some comparisons made by DELCROIX and HENIN (1991) show a close agreement between interpolated and recorded value, except in the vicinity of salinity fronts.

In order to improve the spatial coverage, profiles of salinity transmitted to the TOGA Subsurface Data Centre (Brest) have been added to our data set. In the Gulf of Guinea, we have used measurements taken by ORSTOM research cruises, which contribute to 25% of the whole data set. Figure 1 shows that observations by 1° square are the largest along four shipping tracks: Europe–West Indies–Central America (Track 5); Europe–French Guyana (Track 20); Europe–Brazil (Track 11); Europe–West Africa–South Africa (Track 15). The track numbers are issued from the TOGA Subsurface Data Centre. The observation density is also good in the coastal areas of the Gulf of Guinea.

The seasonal variability has been documented by long term monthly mean charts on a 1° × 1° grid prepared by objective analysis of all the available data (See Appendix).

The year-to-year variability has been documented by objective analysis along the four shipping tracks using a 1° latitude–1 month grid.

THE ANNUAL CYCLE OF THE SSS IN THE WHOLE TROPICAL ATLANTIC

To identify the main causes of SSS variability along the shipping routes and to investigate the year-to-year evolution, a Principal Component Analysis (PCA) is performed on the gridded fields. Also, harmonic analysis of the 12 monthly charts shows that the amplitude of the annual variation reaches its strongest values (Fig. 2A) in four areas: a zonal band near 7–8°N, west of 50°W north of the equator, near the Gulf of Guinea and off the west Africa coast at 11–12°N.

In the zonal band at 7–8°N, the amplitude increases in the vicinity of African and American coasts where it is more than 2.0 p.s.u. off French Guyana. The amplitude, west of 50°W, is due to seasonal fluctuations of the oceanic circulation and of the outflows of the Amazon and Orinoco Rivers. Near the Gulf of Guinea, it is due to the influence of the Congo River. The northwestward tongue from the mouth of the Amazon River may be explained by the northwestward Currents of Brazil and Guyana. From this maximum, the amplitude has a rapid southeastward and northward decrease. It decreases with a smaller gradient east to the African coast.

The part of variance contained in the annual harmonic (Fig. 2C) shows that the large signal corresponding to the fluctuations of Amazon and Congo outflow is relatively noisy near the coast where the dispersion of the SSS values is the greatest. In the Gulf of Guinea, between the equator and 5°S, the strong amplitude has a westward extension, which is probably due to the advection by the South Equatorial Current of the water outflowing the Congo River.

With more than 90% of the variance in the annual harmonic and an amplitude reaching 1.0 p.s.u., the annual signal is most pronounced in the Caribbean area and around the West Indies Arc (Fig. 2C). Between 10 and 15°N it is well defined between 50°W and the African coast and in the greatest part of the Gulf of Guinea (70–80% of the variance extracted). North of 25°N the annual signal is also well defined but with an amplitude less than 0.2.

Minimum SSS occurs (Fig. 2B) in September–October in a 10° wide zonal belt centered at 8°N, from the African coast to 40–45°W and west of 65°W near 20°N. Between these two zones, the minimum occurs earlier. The phase changes abruptly north of this zone where the minimum occurs in February–March. South of this zone, the phase changes gradually with a minimum in May near the equator. In the Gulf of Guinea, the minimum occurs in January in the far east.

The semi-annual signal usually explains less than 50% of the variance, except in small areas as, for example, between the equator and 5°N between 30°W and 15°W, where it may be interpreted as the effect of the double passage of the ITCZ during its annual meridional excursion.

WESTERN TROPICAL ATLANTIC: MAJOR INFLUENCE OF THE RIVER OUTFLOWS

River outflows have a large influence in the Western Tropical Atlantic because of two of the largest outflows in the world ($175–300 \times 10^3$ m^3 s^{-1} for the Amazon River, 20×10^3 m^3 s^{-1} for the Orinoco River), which has already been investigated by RYTHER *et al.* (1967), NEUMANN (1969), FROELICH *et al.* (1978), BORSTADT (1982), MULLER-KARGER *et al.* (1988) and others. However, just how the outflow spreads from the coastal area into the open ocean is not known. In this section, the climatological salinity in the coastal area and open

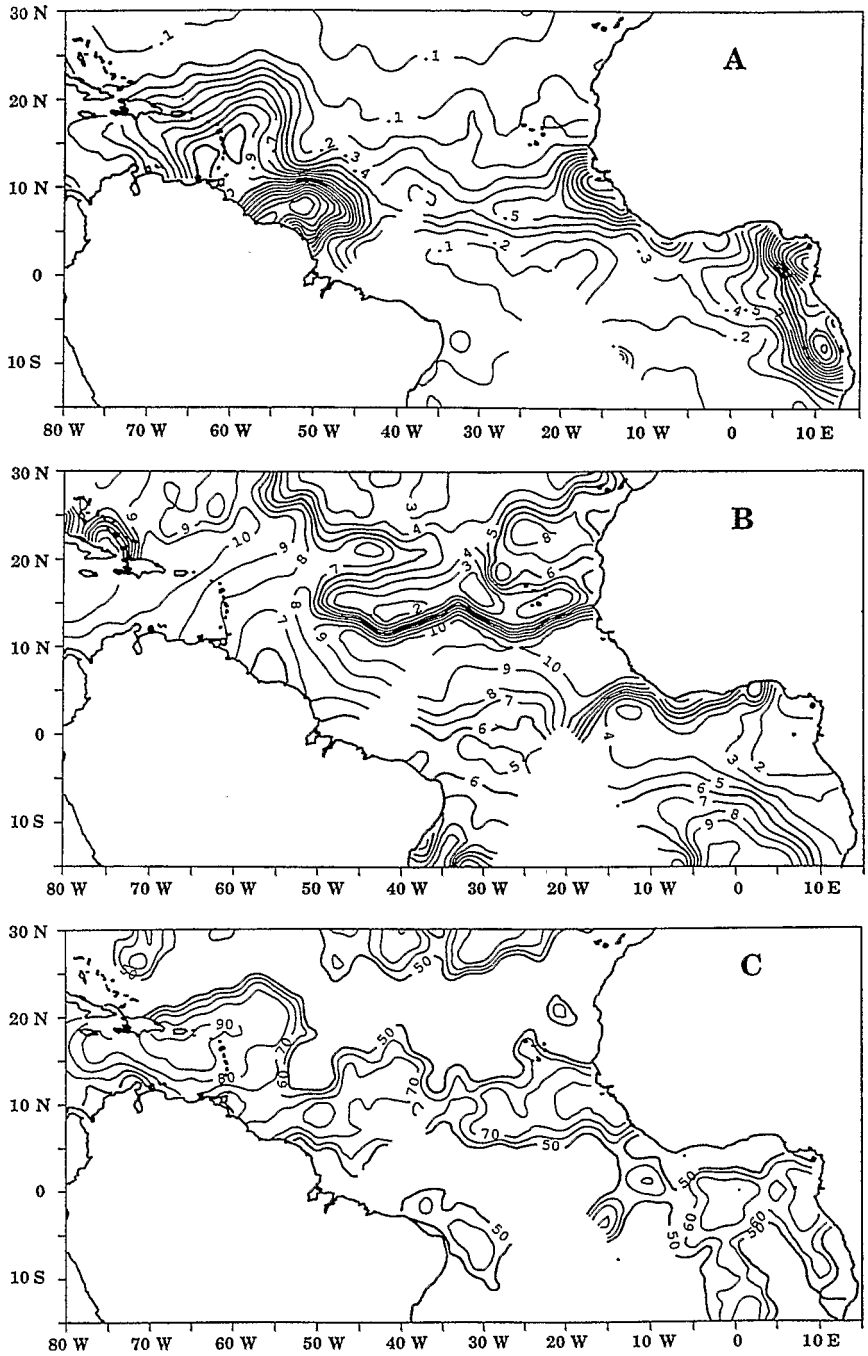

Fig. 2. Harmonic analysis of the annual cycle (set of 12 monthly values). (A) Amplitude of the first harmonic (annual signal). (B) Phase of the first harmonic (month when the annual minimum of SSS is observed). (C) Percentage of variance represented by the first harmonic.

ocean is described, then it is related to outflow of the Amazon and Orinoco River, and finally interannual variations are described.

Coastal area

Near shore (5–6°N, 50°W), the mean cycle shows a SSS minimum in August, after maximum Amazon outflow (Fig. 3A). As the flood of the coastal rivers in French Guyana is concurrent with or slightly precedes that of the Amazon, it is possible that local conditions also have a role in the origin of the SSS annual minimum. Maximum strength of the Guyana Current occurs with the Amazon flood. The current is indicated by the turbid Amazon water near the mouth and identified on GOES visible imagery (CURTIN and LEGECKIS, 1986) extending off the coast of French Guyana during northern summer.

Open ocean

Offshore, the annual signal is clearly defined. The PCA done on the space–time grid relative to the shipping track ending in Cayenne (Track 20) shows that the annual signal (72% of variance) is maximum at about 7°N (50°W) (Fig. 4), 500 km away from the coast, with the amplitude of the mean seasonal cycle reaching 3 p.s.u. (Fig. 3A). In this area, the August average precipitation is less than 150 mm and its role is probably negligible (Yoo and CARTON, 1990) (Fig. 5A). Toward the northeast, from 12°N, the phase of the first harmonic changes quickly and its amplitude decreases (Fig. 2); during the second part of the year, the zone corresponds approximately to the limit between the North Equatorial Current and the North Equatorial Counter Current (RICHARDSON and WALSH, 1986). The rainfall maximum of October–November is well defined and it can be the cause of the simultaneous diminution of the SSS, which culminates in November–December. Between 15°N and 20°N, the SSS seasonal variability is weak, with a minimum between March and June.

Extension of the Amazon waters into the ocean and toward West Indies

The monthly climatological charts (Fig. 6), though giving a very crude picture of the SSS field, show a low SSS plume extending toward the north or northwest during the first part of the year, in contrast with an eastward extending (between 10 and 15°N) low-salinity plume in autumn. This already has been observed by COCHRANE (1969) from hydrological surveys. MULLER-KARGER *et al.* (1988) analysed the spreading Amazon River plume with drifting buoys and CZSC imagery, and noted the role of the retroflexion of the North Brazil Current and the South Equatorial Current, which are the sources of the North Equatorial Countercurrent during the second part of the year (RICHARDSON and REVERDIN, 1986). A part of the Amazon outflow, more or less discontinuously advected eastward by the North Equatorial Countercurrent, participates in the formation of this zonal belt of SSS less than 36.0 p.s.u. which extends all the way from South America to Africa between June and December. The monthly SSS charts (Fig. 6) and the mean cycle suggests low SSS patches in the 5–10°N zonal belt (Fig. 3E) between 30 and 40°W in October–December; although data in this area are scarce, these features may be considered as the most eastern influence of the Amazon water on the SSS.

The bulk of the Amazon waters (extending to at least 30 m depth) spreads north-

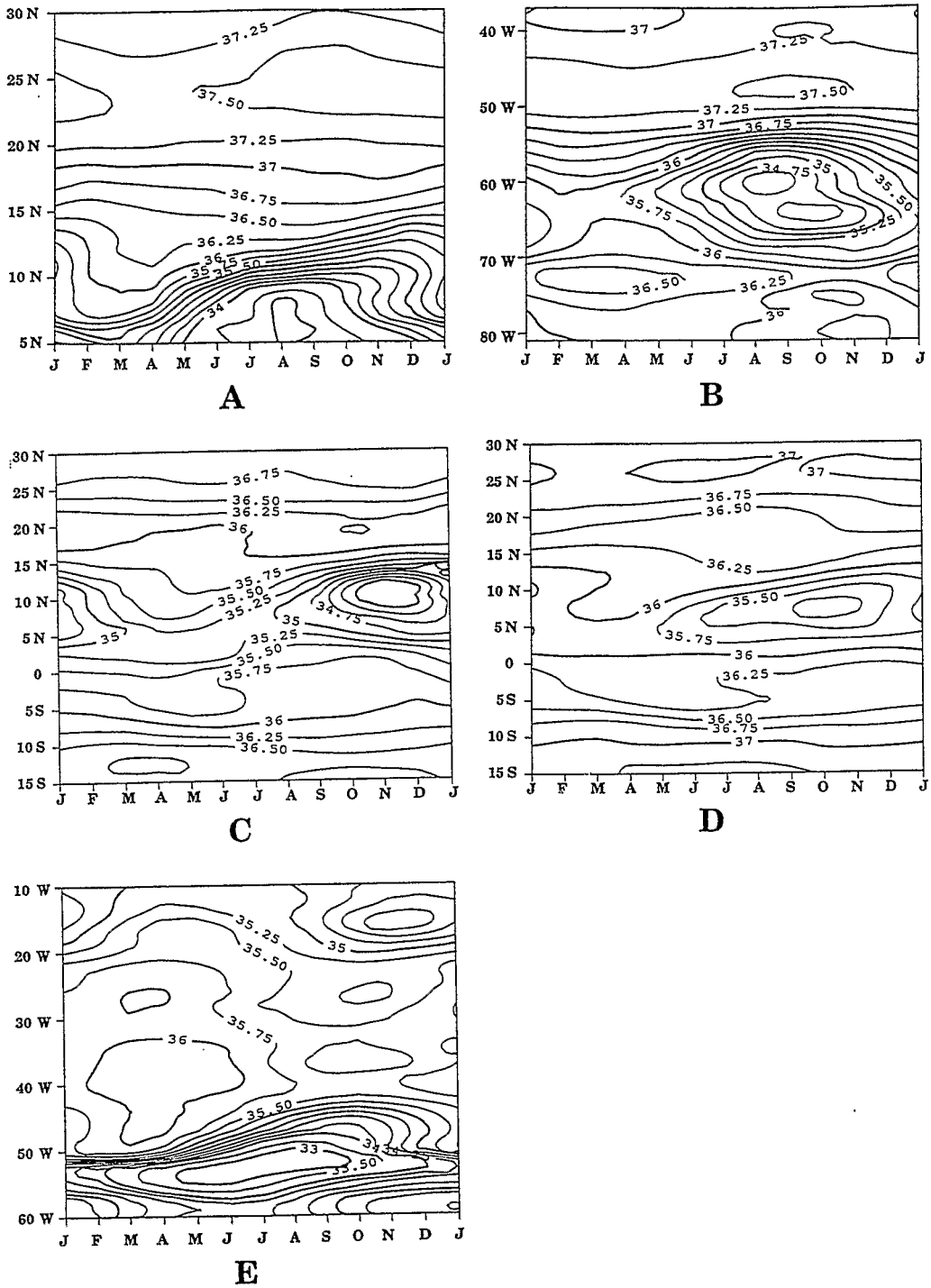

Fig. 3. Mean annual cycles of the SSS (space–time diagram) along the four shipping routes and between 5 and 10°N (1977–1989). (A) Track no. 20 (Europe–French Guyana). (B) Track no. 5 (Europe–West Indies). (C) Track no. 15 (Europe–West Africa–South Africa). (D) Track no. 11 (Europe–Brazil). (E) Zonal belt 5°N–10°N.

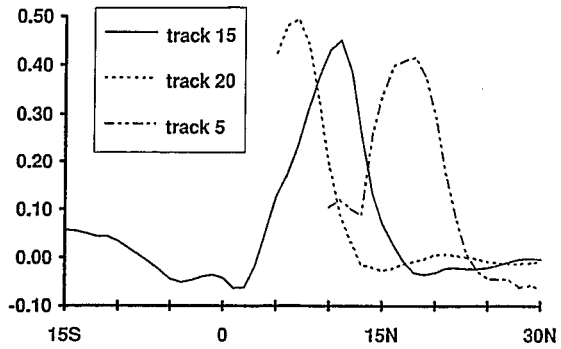

Fig. 4. First factors (annual signal) extracted by PCA done on the space–time grid relative to the Tracks 5, 15 and 20.

westward into the Guyana Current and is finally advected by the North Equatorial Current toward the West Indies. Moreover, from January to June, the North Equatorial Countercurrent is replaced by westward drift (ARNAULT, 1987) due to the influence of the Guyana Current (RICHARDSON and WALSH, 1986). Consequently, most of the Amazon water flows northwestward and westward, contributing to the seasonal variability of the SSS in the Caribbean area (FROELICH *et al.*, 1978). The amount of the advection of the Amazon waters, north of 7–8°N, depends on the fluctuations of Amazon outflow as well as the initiation of the North Equatorial Countercurrent. In the northwestern area of the tropical Atlantic, the annual signal is particularly clear, with a SSS minimum occurring at the end of the summer.

The first factor extracted by PCA, performed on the grid relative to the Track 5 (Europe–West Indies), represents 67% of the SSS variance and can be identified as the seasonal signal that has an intensity maximum between 16 and 18°N (57–60°W) (Fig. 4). The associated temporal orthogonal function usually shows a minimum in September. In the early part of the year, the SSS monthly climatology shows the presence of low salinity water at the same time that Amazon outflow increases. In June, the patch extends from the Amazon mouth to about 20°N. Beginning in July, it is separated in two parts by a high salinity tongue off Guyana and roughly aligned southwest–northeast. The Guyana Current is then the strongest whereas, according to MAZEIKA (1973), the West Indies Arc could induce a southward deflection of the North Equatorial Current (VAN BENNEKOM and TIJSSEN, 1978). According to METCALF (1968), this would lead to a partial reversal of the Guyana Current. Some events confirm such a scenario: in July, the ITCZ reaches its northernmost (8°N) location, and, on the South America coast, the southeast trade winds induce upwelling (GIBBS, 1980) capable of bringing saltier waters from the north–northwest to the surface.

The Caribbean Sea and the outflow of the Orinoco River

In the Caribbean area (65–70°W), SSS has a different cycle than rainfall (Figs 3B and 5B) and it is therefore likely that rainfall plays a minor role in SSS evolution, compared to the seasonal arrival of the Amazon waters in July when the Guyana Current is fast enough (1.5–2 knots) to bring these waters to the West Indies Arc in 3–4 weeks.

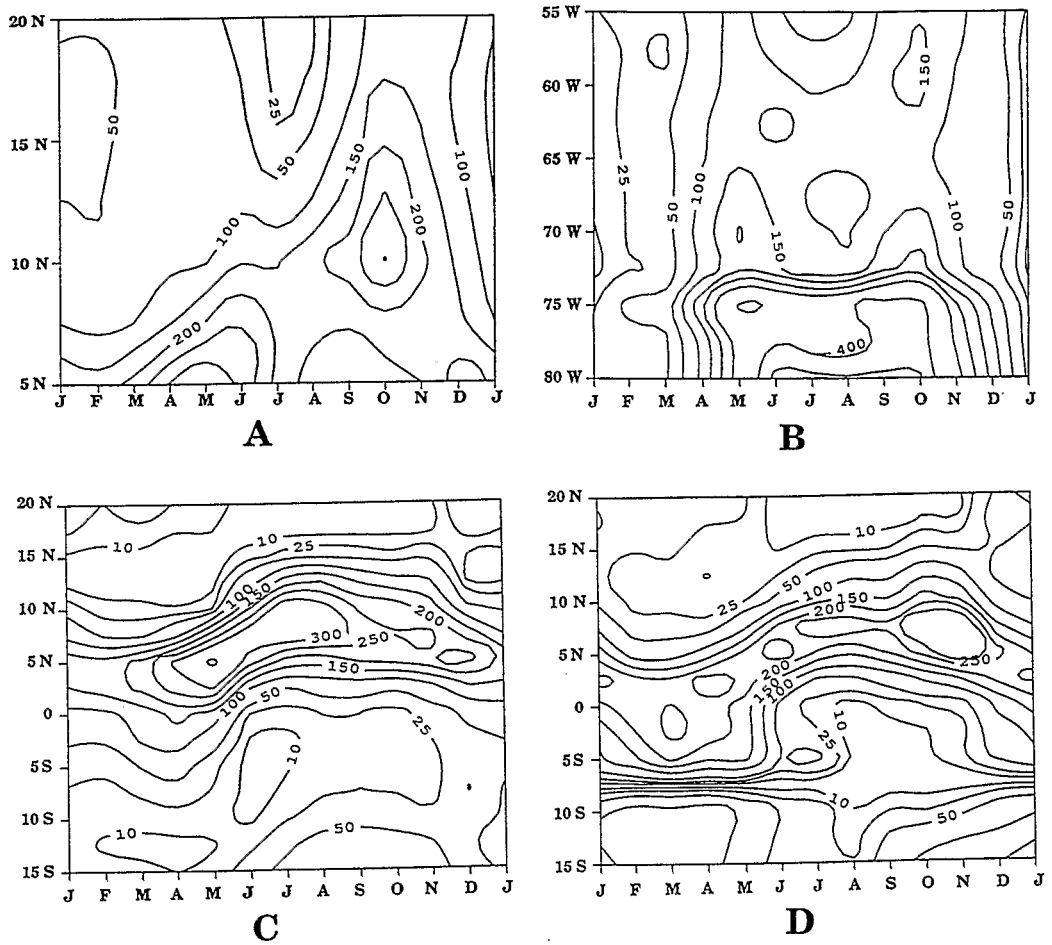

Fig. 5. Mean annual cycles of rainfall (mm/month) from Yoo and CARTON (1990) along the four shipping routes (1974–1985). (A) Track no. 20 (Europe–French Guyana). (B) Track no. 5 (Europe–West Indies). (C) Track no. 15 (Europe–West Africa–South Africa). (D) Track no. 11 (Europe–Brazil).

The Orinoco River, with a flow 7–8 times weaker than the Amazon, has its flood in August–September (GADE, 1961), about 2 months after the Amazon. Its waters, advected by the North Equatorial Current, flow out mainly into the Caribbean Sea (SSS is minimum in August–September with 1.5 p.s.u. amplitude). Along Track 5 (Europe–West Indies), the first factor extracted by PCA has a main peak at 59°W east of the West Indies Arc when the SSS is minimum in August–September with a mean amplitude of 1.9 p.s.u. A smaller peak occurs at 64°W in the Caribbean Sea, where the SSS is minimum in September–October with an amplitude of 1.5 p.s.u. These two minima shift in time and space relative to the mean cycle (Fig. 3B) which could be interpreted as the successive arrivals of water from the Amazon and Orinoco River, in agreement with FROELICH *et al.* (1978) who have shown that variations of SSS occur simultaneously in the whole Venezuelan basin.

In the Caribbean Sea, the Caribbean Current fed by the North Equatorial Current and the Guyana Current (GORDON, 1967) flows zonally at about 13–14°N with a small seasonal variability. For FROELICH *et al.* (1978), the advection of Amazon water into the Caribbean Sea and the progress of the low salinity during the second part of the year are due to this circulation system. East of 70°W, the shipping track is exactly located along the axis of the Caribbean Current, and the amplitude of the seasonal variations of the SSS as well as the fluctuations scenario seems to confirm the hypothesis of FROELICH *et al.* (1978).

In the west of the Caribbean Sea, the shipping track becomes closer to the shore where coastal upwelling brings saltier water to the surface. The amplitude of the seasonal fluctuations of the SSS decreases (Fig. 3B). The regular freshening, which starts in April–May, coincides with the rainy season (Fig. 5B). Consequently, west of 70°W, the local conditions induce the greatest part of the seasonal variability of the SSS with a great instability of the annual minimum. Globally, the freshwater balance of the Caribbean Sea shows a deficit ranging from 74 to 104 cm y^{-1} (ETTER *et al.*, 1987; YOO and CARTON, 1990). With the intake of the river outflows, YOO and CARTON (1990) bring down the estimation from 74 to 39 cm.

Year-to-year variability

Along Track 20 (Europe–French Guyana), the extreme spatial variability masks annual and interannual signals, except in the area of SSS maximum (20–30°N, 20–50°W, Fig. 3A) where there are weak but noise-free seasonal variations. Between 1977 and 1982, annual maximum increases, but the minimum remains almost the same.

Along Track 5 (Europe–West Indies) (Fig. 3B), the long transit of the low salinity waters from the Amazon has homogenized the mixed layer. In the West Indies area, the annual cycle (Fig. 2C) is not disturbed but there is no clear year-to-year trend. However, it seems that the spring decrease of the SSS has shifted to a later time through the year, and that, north of 15°N, a small increasing trend for the monthly anomalies appears. ROGERS (1988) has pointed out correlations of the year-to-year variations of the rainfall in tropical America with the Southern Oscillation (SO). For example, during weak SO and El Niño, the precipitation would be significantly weaker than during a cold event. According to HASTENRATH (1990), precipitation in northern South America is particularly correlated to the Southern Oscillation Index (SOI). Between November 1982 and April 1983, the anomalously south location of the Intertropical Convergence Zone (ITCZ) in the east Pacific induced in the southwest of the Caribbean Sea a 50% deficit of precipitation; as this period was not the rainy season, there was no response of the SSS. However, the year-to-year variations of the Amazon regime could be connected to change of the atmosphere circulation in the tropical Pacific associated with El Niño–Southern Oscillation (ENSO) phenomenon. RICHEY *et al.* (1989) observe that ENSO events often precede negative anomalies of discharge, as for the 1925–1926 and 1982–1983 major events. The opposite phases (cold events or La Niña) are related to an increase of the discharge. According to HASTENRATH (1990), a strong discharge of the rivers in northern South America is connected to a northward ITCZ motion characterized by a high SOI during the northern winter. So, along the Track 5, off the West Indies, the SSS minimum in summer 1983 is least pronounced during the 1977–1986 period. Unfortunately, after 1986, the density of observations was too low to observe the effect of the 1986–1987 ENSO as well as the 1989–1990 cool period.

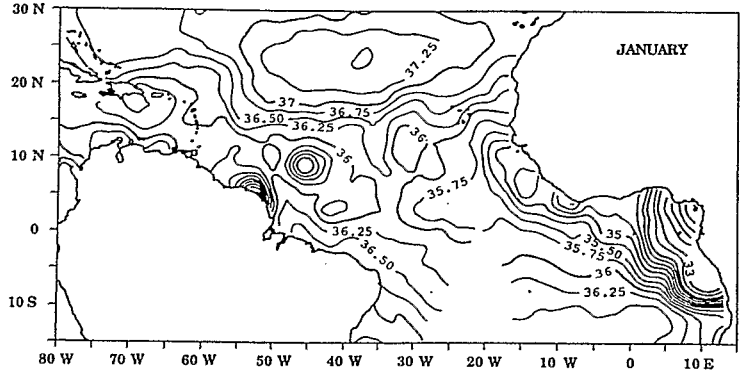
JANUARY
30 N
20 N
10 N
0
10 S
80 W
70 W
60 W
50 W
40 W
30 W
20 W
10 W
0
10 E
37.25
37
36.75
36.50
36.25
36
35.75
35.50
35
34
33

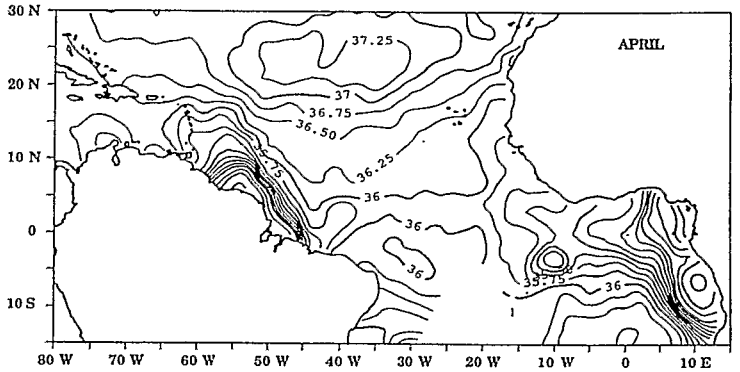
APRIL
30 N
20 N
10 N
0
10 S
80 W
70 W
60 W
50 W
40 W
30 W
20 W
10 W
0
10 E
37.25
37
36.75
36.50
36.25
36
35.75

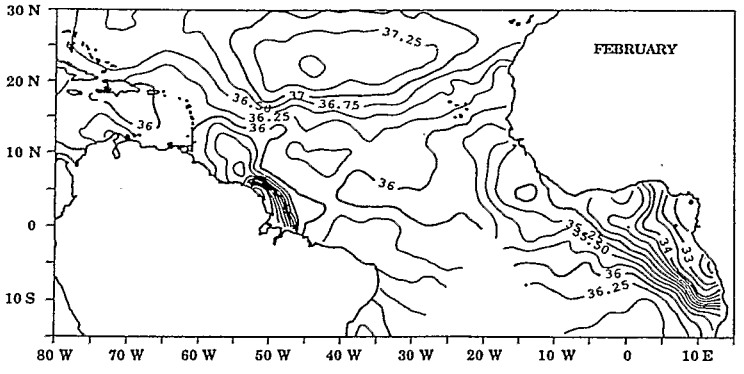
FEBRUARY
30 N
20 N
10 N
0
10 S
80 W
70 W
60 W
50 W
40 W
30 W
20 W
10 W
0
10 E
37.25
37
36.75
36.50
36.25
36
35.50
34
33

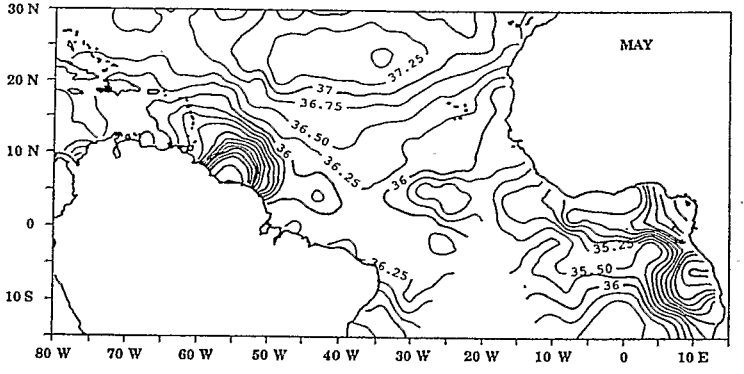
MAY
30 N
20 N
10 N
0
10 S
80 W
70 W
60 W
50 W
40 W
30 W
20 W
10 W
0
10 E
37.25
37
36.75
36.50
36.25
36
35.50

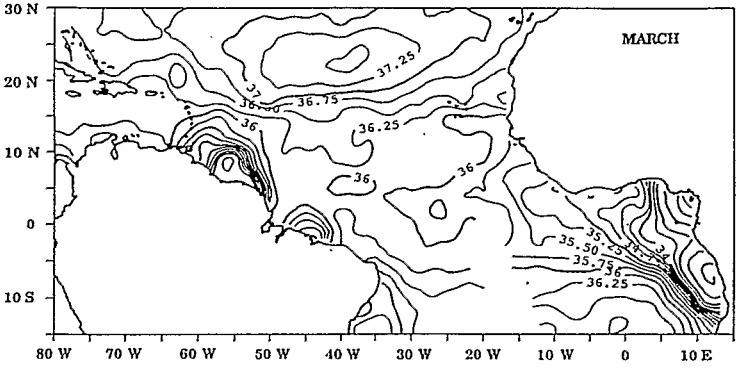
MARCH
30 N
20 N
10 N
0
10 S
80 W
70 W
60 W
50 W
40 W
30 W
20 W
10 W
0
10 E
37.25
36.75
36.25
36
35.75
35.50
34

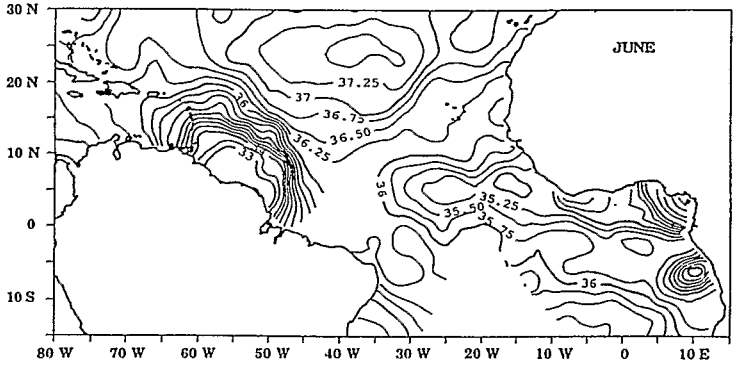
JUNE
30 N
20 N
10 N
0
10 S
80 W
70 W
60 W
50 W
40 W
30 W
20 W
10 W
0
10 E
37.25
37
36.75
36.50
36.25
36
35.50
35.25
35.75

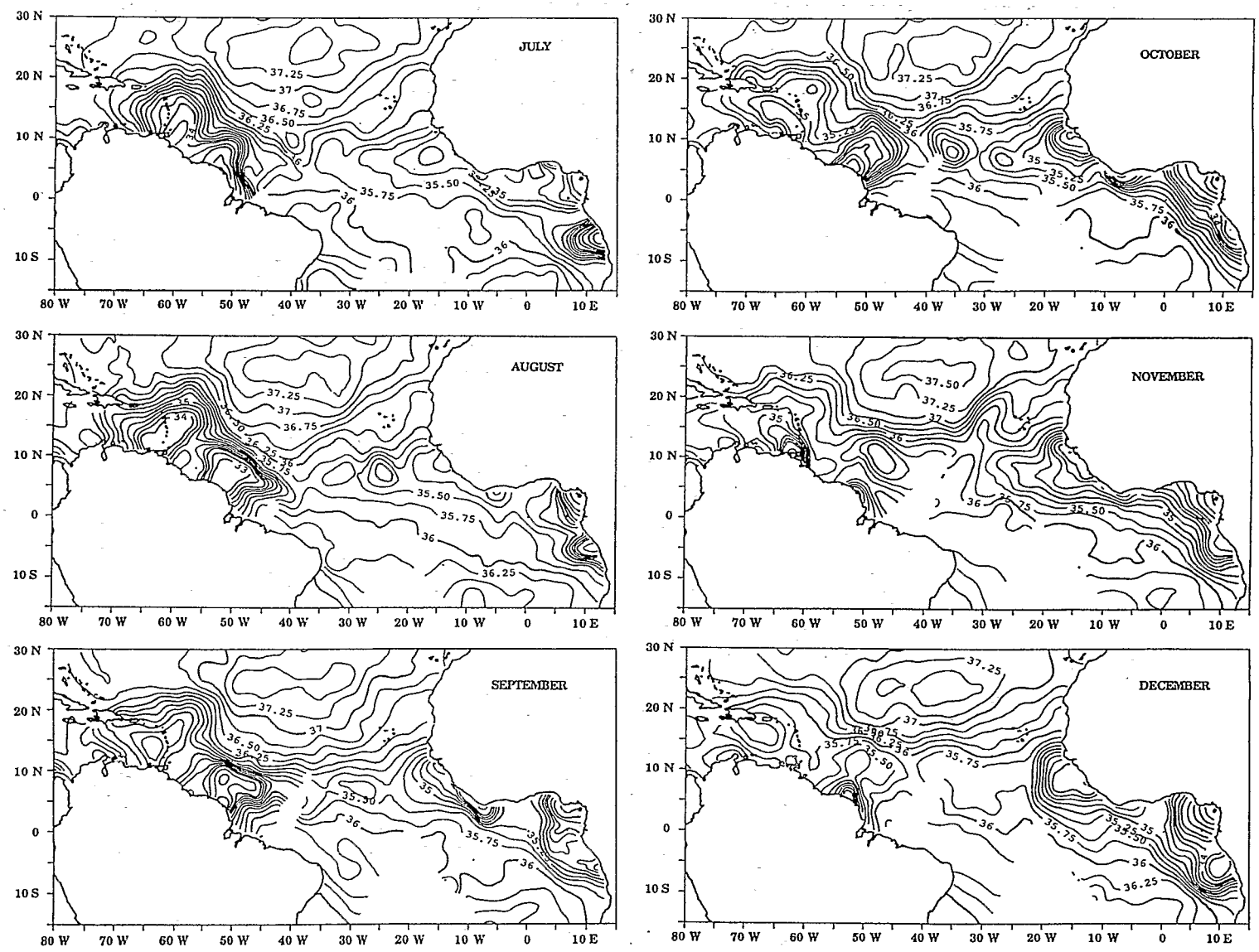

Fig. 6. Monthly climatology of the SSS.

EASTERN AND CENTRAL TROPICAL ATLANTIC—ROLE OF THE ITCZ AND THE PRECIPITATIONS

In this section, the seasonal variability of SSS is related to the evaporation–precipitation balance and to the movement of the ITCZ. Then, the year-to-year variability is investigated with particular reference to the anomalous 1984–1985 years.

Seasonal variability (Fig. 3C, 3D)

East of 35–40°W, in the zonal SSS minimum at 8°N, the local evaporation–precipitation balance becomes the main cause of the variability. According to climatological charts of precipitation (DORMAN and BOURKE, 1981), there is a zonal precipitation maximum between the equator and 10–12°N. In northern winter during the rainy season, a zonal decreasing gradient of rainfall appears off the coast of Africa. During autumn, the rainfall maximum moves westward and in November is located between 20 and 40°W. Low salinity patches (Fig. 6) are found in the middle of the Atlantic, particularly in autumn. These patches may consist of lenses of Amazon waters advected eastward by the North Equatorial Countercurrent which has, at this time, its maximum intensity. Along Track 15 (Europe–South Africa), at 150°W, the meridional movement of the SSS minimum is almost 7° latitude during the year (Fig. 3C). The amplitude decreases westward and is only 4–5° latitude along Track 11 (Europe–Brazil) (Fig. 3D) between 25 and 30°W. The minima of SSS are approximately in phase along these two tracks; on the western track, the greatest persistence of this minimum may be connected to the double passage of the ITCZ (June–July and October–November) during its meridional movement (Fig. 5D).

Year-to-year variability

The salient feature of the year-to-year variability is the strong decrease of the seasonal amplitude in 1984 and 1985, as represented by the first component (64% of the variance) obtained by the PCA made on the observations along the Track 15 (Europe–West Africa). Its intensity is maximum about 10–11°N (Fig. 4), and in 1984–1985 the amplitude of the signal is only 60% of the 1977–1989 average (Fig. 7A). The autumn minimum in November 1985 is particularly smoothed with a positive anomaly of almost 2.0 p.s.u. (Fig. 7B); the spring maximum for 1984 and 1985 is the highest of the time series.

Along Track 15 (Europe–West Africa), between 10°S and 20°N, the SSS increased during the 1977–1985 period reaching a value observed until 1989 (Fig. 8). The trend affects both the annual maxima and minima. The PCA on the grid of the monthly deviations relative to a standard year shows that deviation and amplitude of the annual signal reach a maximum at about 10°N; the first factor representing this trend extracts 42% of the variance.

Unusual conditions prevailed in the tropical Atlantic in 1984 (PHILANDER, 1986; LAMB *et al.*, 1986; HISARD *et al.*, 1986; and others). At 3°N, 10°W the phase of the seasonal signal reversed (minimum in April–March instead of July) (Fig. 2), whereas in the equatorial zone, the annual variability of the SSS was maintained. In 1984 and 1988 the upwelling intensity was weak, but the SSS response for these both years was not significant (Fig. 8). Similarly, precipitation, which in March–April 1984 was twice the average, apparently did not change the SSS minimum. As year-to-year variability of the upwelling and the

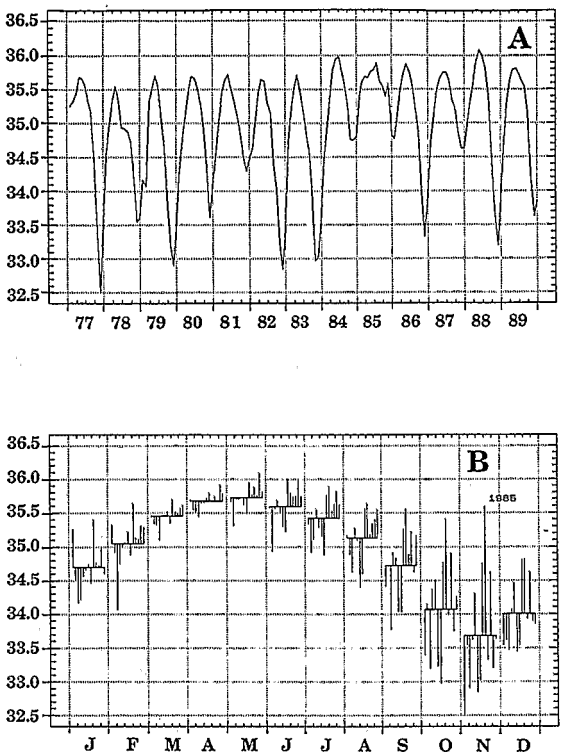

Fig. 7. (A) Evolution of the SSS along the Track 15 (Europe–West Africa) at 10°N. (B) Mean annual cycle; the vertical lines represent the deviations relative to the monthly means for each year of the set.

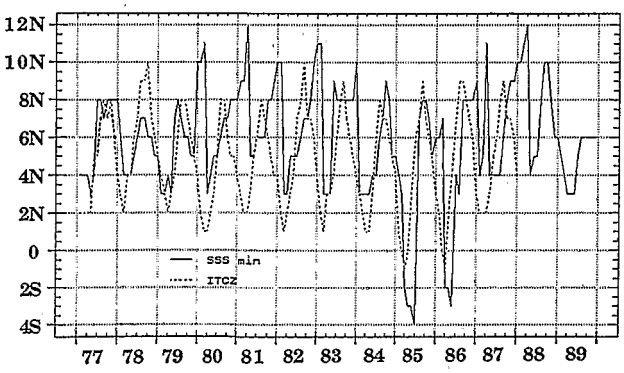

Fig. 8. Evolution of the mean anomalies of the SSS between 10°S and 20°N along the shipping route no. 15 (Europe–West Africa).

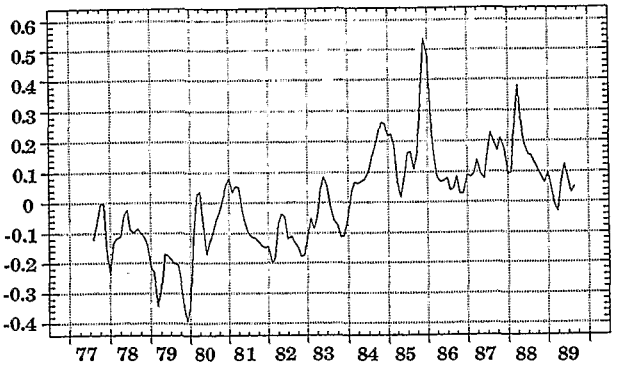

Fig. 9. Location in latitude of the monthly minimum of the SSS and of the Intertropical Convergence Zone (ITCZ) along the Track no. 11 (Europe–Brazil).

precipitation was not concomitant with the SSS variability, it seems that the general warming trend (SERVAIN, 1991) observed during the studied period was accompanied by SSS increase reaching a plateau in 1985–1986 (Fig. 8).

In the Southern Hemisphere, the seasonal signal also was reversed (Fig. 2B). A year-to-year variability remains, as pointed out by the PCA applied in the southern part of the Track 15 (Europe–South Africa), and at 9°S, in the South Equatorial Current, this factor has the largest loading. In 1984 and 1985, the function associated with the second factor shows a clear peak corresponding to positive SSS anomalies. The cause is probably the large interannual fluctuations of the Congo River flow (40×10^3 m^3 s^{-1}). The seasonal floods of December 1983 and December 1984 were clearly weaker than the average, and it is likely that this deficit of the freshwater discharge has some consequences on the SSS advected westward by the South Equatorial Current. However, the oceanic zone, where the SSS is affected by the Congo outflow, is relatively restricted and imperfectly separated from fresh waters originating from the Bay of Biafra (Fig. 6).

The Track 11 (Europe–Brazil) (Fig. 9), between Brazil and Cape Verde Islands, in the open ocean, also shows a SSS increase between 1977 and 1984–1985, mostly north of the Equator. However, the amplitude of the signal has not changed interannually despite this SSS increase.

The ITCZ reaches usually its northernmost location (8°N) in August (HASTENRATH and LAMB, 1977; CITEAU *et al.*, 1988), and at a given longitude precedes by about 2 months the northernmost location of the SSS. In contrast (Fig. 9), in March 1985 and 1986, the southernmost position of the ITCZ has exceeded by almost 2.5° latitude the mean location for this particular month (CITEAU *et al.*, 1988). This event induced strong rainfall in the north-east of Brazil, with the greatest Hastenrath index observed in 1985 since 1912, and a particularly southern location of the SSS minimum in 1985–1986 (Fig. 9).

In 1982–1983, the tropical Pacific was struck by a very strong anomaly (ENSO) and this feature was invoked to explain the atmospheric oceanic patterns observed in the tropical Atlantic in 1983–1985. So, between 20 and 35°W the small OLR (Outgoing Longwave Radiation) intensity in February–March 1983 is connected between 5°S and the equator to a decrease of the precipitation (HOREL *et al.*, 1986). The response of the SSS in the 0–5°S belt, Track 11, is a seasonal minimum in April–May 1983 which is the least noticeable of the 1977–1985 period.

RELATION BETWEEN SSS AND FRESHWATER BALANCE

The value of the SSS is directly related to the freshwater balance at the ocean surface. The Atlantic Ocean receives freshwater through the precipitation (P) and to a lesser extent from the river discharge (R); it loses it through evaporation (E). The sum of these terms, which represents the freshwater flux (F) to the ocean surface: $F = (P - E) + R$, can be calculated by using direct method (P, E and R are estimated separately), (e.g. BAUMGARTNER and REICHEL, 1975). The annual and year-to-year variability of this flux in the tropical Atlantic and the Caribbean Sea has been studied by Yoo and CARTON (1990). The importance of the different terms used in the F calculation fluctuates according to the period of the year and the geographical location. Without advection of water of continental origin, in a first estimate, a negative correlation is expected between the SSS and the local balance $P - E$, which may be represented schematically by a linear regression. With a negative $P - E$ balance (more evaporation than precipitation) there is a positive deviation relative to the regression. Conversely, the advection of continental waters would induce a negative deviation. By consideration of these deviations, it is possible to distinguish roughly the geographical zones and the period of the year where one factor determines SSS.

The 11 years of the monthly fields estimated by Yoo and CARTON (1990) from OLR have been used to build a monthly climatology (Fig. 5). The files of HASTENRATH and LAMB (1978) have been used to estimate the evaporation. The monthly climatology of $P - E$ balance has been calculated from these two data sets. For the twelve monthly climatology fields, the SSS regression in function of the $P - E$ balance of the previous month is estimated, and then the deviations of the observed values relative to the values issued from the regression are calculated. Figure 10 presents a quarterly mapping of these residuals. During the first quarter of the year, the continental influences on the SSS are the strongest in the Gulf of Guinea (with a plume in the south corresponding to the main flood of the Congo in December and continuing to the North with the permanent low SSS area in the Bay of Biafra). In the west, the influence of the Amazon River is very weak during the northern winter but, during the spring, occurs strongly at the East of the West Indies Arc; in the Gulf of Guinea, the impact of the Congo, which at this time is well separated from the Bay of Biafra, is decreasing. During northern summer, the continental influence reaches the Caribbean Sea (because of the Orinoco flood), whereas the initial eastward drift of the Amazon waters with the North Equatorial Counter Current is sensed between 5 and 10°N. During the last quarter of the year, the continental influences are decreasing in the west, whereas, off the African coast, they reach the western Africa where the floods of the coastal rivers have occurred in August–September. It seems also that at this time of the year, the influence of the evaporation on the SSS is the strongest north of 15°N.

LONG-TERM EVOLUTION OF THE SSS

North of the equator (15–25°N on Track 11, Europe–Brazil) a certain trend to the increase of SSS during the last 10 years has been observed (Fig. 11). LEVITUS (1989), comparing the mean SSS during two periods, 1955–1959 and 1970–1974, has noticed an increase of the SSS significant at 99% at about 25–30°N and 50–20°W (area of the SSS maximum core). In the same area, the annual climatology calculated by LEVITUS (1982), does not show SSS more than 37.5 p.s.u., whereas, during the 1977–1989 period, an SSS core larger than 37.5 is observed about 25°N and 30–40°W. However, the difference of

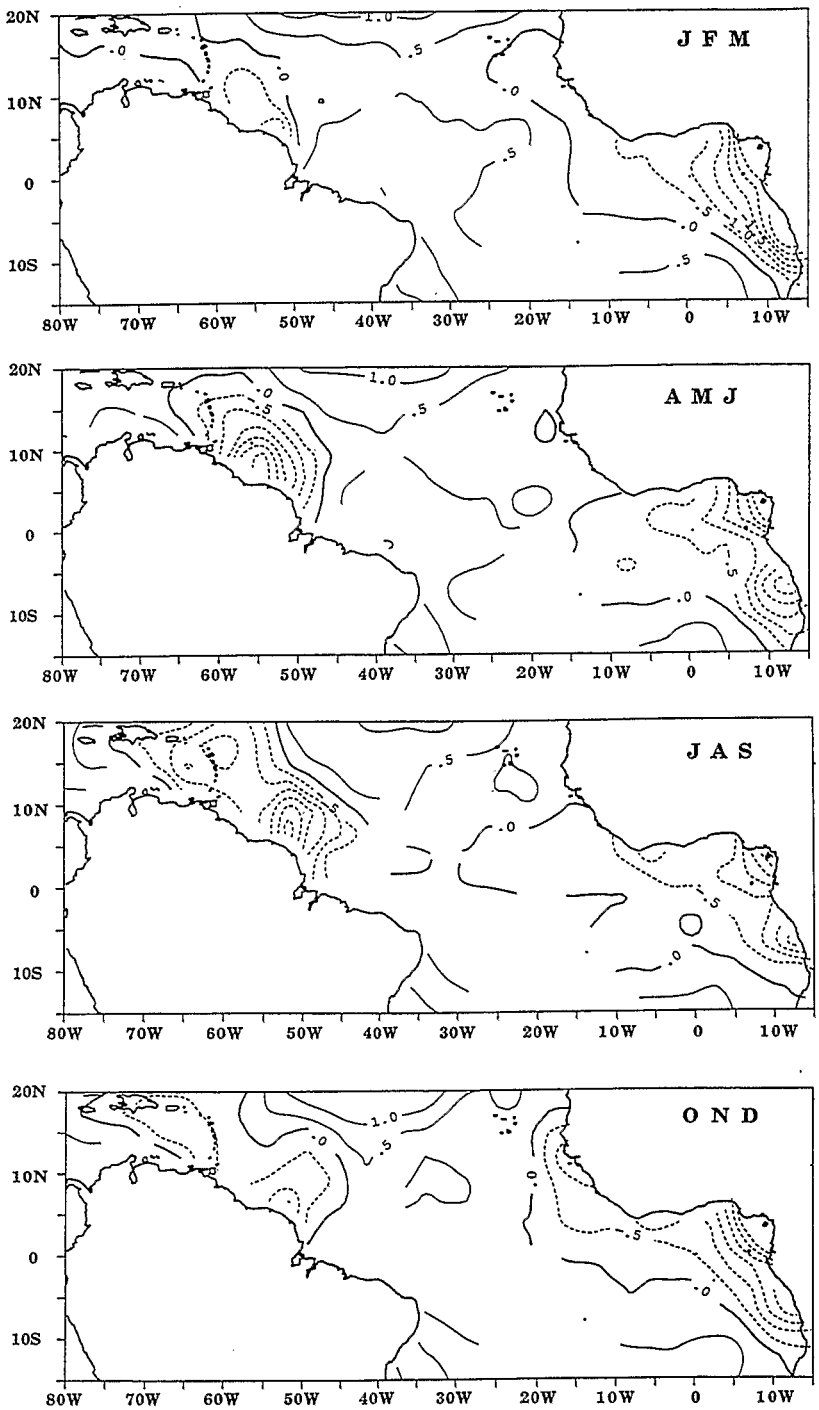

Fig. 10. Quarterly location of the deviations between observed values of the SSS and the estimated values from a regression between SSS and precipitation–evaporation balance.

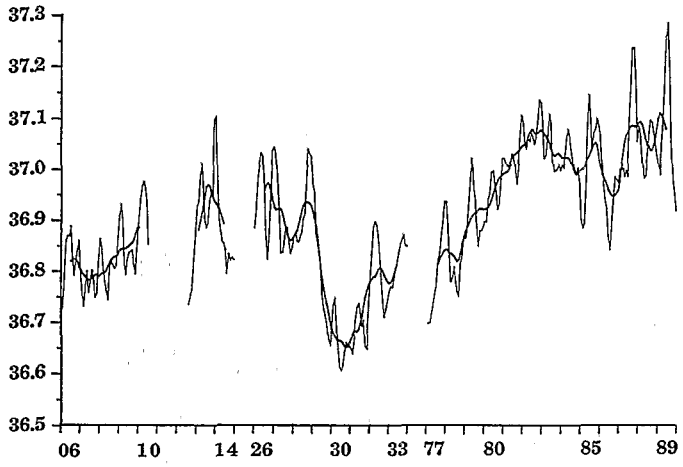

Fig. 11. Evolution of the SSS between 25 and 29°N (Track no. 11) during three periods: 1906–1914, 1926–1933 (from SMED) and 1977–1989.

origin and of analysis of these data sets suggests caution in accepting this apparent increase. SMED (1943), in order to analyse the seasonal variability of the SSS in the north Atlantic, has also used surface observation gathered by ships of opportunity beginning in 1902. Some data come from Track 11 and the sampling during two periods 1906 and 1914, and 1926 and 1933 is sufficient to follow the SSS evolution between 25 and 29°N (15–20°W, Fig. 11). During these periods and also from 1977 to 1980, the monthly means are not more than 37.0, whereas starting in 1980, values of more than 37.0 are prevailing. So, it seems that, in the East of the North Tropical Atlantic, there is a clear increase of the SSS, perhaps unprecedented since the beginning of the century.

Acknowledgements—The authors wish to thank the officers and the crew of numerous merchant ships who voluntarily participated in this surface salinity experiment. They are also grateful to Michel Prive and Robert Gerard who greeted most of these ships.

REFERENCES

ARNAULT S. (1987) Tropical Atlantic geostrophic currents and ship drifts. *Journal of Geophysical Research*, **92**, 5076–5088.

BAUMGARTNER A. and E. REICHEL (1975) *The world water balance: mean annual global, continental and maritime precipitation, evaporation and run-off*. Elsevier, 179 pp., 31 pp. maps.

BERRIT G. (1961) Contribution a la connaissance des variations saisonnieres dans le golfe de Guinee. Observations de surface le long des lignes de navigation—1ere partie: generalities. *Cahiers Oceanogr. (Bull. COEC)*, **13**, 715–727.

BERRIT G. (1962) Contribution a la connaissance des variations saisonnieres dans le golfe de Guinee. Observations de surface le long des lignes de navigation—2eme partie: etude regionale. *Cahiers Oceanogr. (Bull. COEC)*, **14**, 633–644.

BORSTAD G. A. (1982) The influence of the meandering Guiana Current and Amazon River discharge on surface salinity near Barbados. *Journal of Marine Research*, **40**, 421–434.

CITEAU J., J. C. BERGES, H. DEMARCQ and G. MAHE (1988) The watch of ITCZ migrations over the tropical Atlantic ocean as an indicator in drought forecast over the sahelian area. *Tropical Ocean–Atmosphere Newsletter*, **45**, 1–3.

COCHRANE J. D. (1969) Low sea-surface salinity off northeastern South America in summer 1964. *Journal of Marine Research*, **27**, 327–334.

CURTIN T. B. and R. V. LEGECKIS (1986) Physical observations in the plume region of the Amazon River during peak discharge. 1° Surface variability. *Continental Shelf Research*, **6**, 31–51.

DELCROIX T. and C. HENIN (1991) Seasonal and interannual variations of sea surface salinity in the tropical Pacific Ocean. *Journal of Geophysical Research*, **96**, 22135–22150.

DONGUY J. R., C. HENIN and R. GERARD (1980) Tropical Atlantic surface salinity. *Tropical Ocean–Atmosphere Newsletter*, 12.

DORMAN C. E. and R. H. BOURKE (1981) Precipitation over the Atlantic ocean, 30°S to 70°N. *Monthly Weather Review*, **109**, 554–563.

ETTER P. C., P. J. LAMB and D. H. PORTIS (1987) Heat and freshwater budgets of the Caribbean Sea with revised estimates for the central american seas. *Journal of Physical Oceanography*, **17**, 1232–1248.

FROELICH P. N., D. K. ATWOOD and G. S. GIESE (1978) Influence of Amazon River discharge on surface salinity and dissolved silicate concentrations in the Caribbean Sea. *Deep-Sea Research*, **25**, 735–744.

GADE H. G. (1961) On some oceanographic observation in the southeastern Caribbean Sea and the adjacent Atlantic ocean with special reference to the influence of the Orinoco River. *Bol. Inst. Oceanogr. Univ. Oriente*, **1**, (2), 287–342.

GIBBS R. J. (1980) Wind-controlled coastal upwelling in the western equatorial Atlantic. *Deep-Sea Research*, **27**, 857–866.

GOHIN F. and G. LANGLOIS (1991) Atlas mensuel des temperatures moyennes dans le Golfe de Gascogne. *Oceanologica Acta*, **14**, 181–187.

GORDON A. J. (1967) Circulation of the Caribbean Sea. *Journal of Geophysical Research*, **22**, 6207–6223.

HASTENRATH S. (1990) Diagnostics and prediction of anomalous river discharge in northern South America. *Journal of Climate*, **3**, 1080–1096.

HASTENRATH S. and P. J. LAMB (1977) Climatic atlas of the tropical Atlantic and the eastern Pacific ocean. University of Wisconsin Press, 112 pp.

HASTENRATH S. and P. J. LAMB (1978) Heat budget atlas of the tropical Atlantic and eastern Pacific oceans. University of Wisconsin Press, 103 pp.

HERZFELD U. C. (1992) Quantitative spatial models of Atlantic primary productivity: an application of geomathematics. *Journal of Geophysical Research*, **97**, 717–732.

HISARD P., C. HENIN, R. HOUGHTON, B. PITON and P. RUAL (1986) Oceanic conditions in the tropical Atlantic during 1983 and 1984. *Nature*, **332**, 243–245.

HOREL J. D., V. E. KOUSKY and M. T. KAGANO (1986) Atmospheric conditions in the Atlantic sector during 1983 and 1984. *Nature*, **322**, 248–251.

LAMB P. J., R. A. PEPPLER and S. HASTENRATH (1986) Interannual variability in the tropical Atlantic. *Nature*, **322**, 238–240.

LEVITUS S. (1982) Climatological atlas of the World Ocean. NOAA Prof. Pap. No. 13, U.S. Govt. Printing Office, 173 pp.

LEVITUS S. (1986) Annual cycle of salinity and salt storage in the World Ocean. *Journal of Physical Oceanography*, **16**, 322–343.

LEVITUS S. (1989) Interpentadal variability of salinity in the upper 150 m of the North Atlantic Ocean, 1970–1974 versus 1955–1959. *Journal of Geophysical Research*, **94**, 9679–9685.

MATHERON G. (1971) The theory of generalized variables and its applications. *Cahiers du Centre de Morphologie methematique n°7*, 175 pp.

MAZEIKA P. A. (1973) Circulation and water masses east of the Lesser Antilles. *Dtsch. Hydrogr. Z.*, **26**, 51–73.

METCALF W. G. (1968) Shallow currents along the northeastern coast of South America. *Journal of Marine Research*, **26**, 232–243.

MULLER-KARGER F. E., C. R. MCCLAIN and P. L. RICHARDSON (1988) The dispersal of the Amazon's water. *Nature*, **333**, 56–59.

NEUMANN G. (1969) Seasonal salinity variations in the upper strata of the western tropical Atlantic ocean. 1. Sea surface salinities. *Deep-Sea Research*, **16**, (Suppl.), 165–177.

NEUMANN G., W. H. BEATTY and E. C. ESCOWITZ (1975) Seasonal changes of oceanographic and marine climatological conditions in the equatorial Atlantic. Unpublished report, SUNY Institute of Marine and Atmospheric Science, 211 pp.

PHILANDER S. G. H. (1986) Unusual conditions in the tropical Atlantic ocean in 1984. *Nature*, **322**, 236–238.

RICHARDSON P. L. and G. REVERDIN (1986) Seasonal cycle of velocity in the Atlantic North Equatorial Countercurrent as measured by surface drifters current meters and ship drift. *Journal of Geophysical Research*, **92**, 3691–3708.

RICHARDSON P. L. and D. WALSH (1986) Mapping climatological seasonal variations of surface currents in the tropical Atlantic using ship drifts. *Journal of Geophysical Research*, **91**, 10537–10550.

RICHEY J. E., C. NOBRE and C. DESSER (1989) Amazon River discharge and climate variability: 1903–1985. *Science*, **246**, 101–103.

ROGERS J. C. (1988) Precipitation variability over the Caribbean and tropical Americas associated with the Southern Oscillation. *Journal of Climate*, **1**, 172–182.

RYTHER J. H., D. W. MENZEL and N. CORWIN (1967) Influence of the Amazon River outflow on the ecology of the western tropical Atlantic. 1. Hydrography and nutrient chemistry. *Journal of Marine Research*, **25**, 69–83.

SERVAIN J. (1991) Simple climatic indices for the tropical Atlantic Ocean and some applications. *Journal of Geophysical Research*, **96**, 15137–15146.

SMED J. (1943) Annual and seasonal variations in the salinity of the North Atlantic surface waters. *Conseil Permanent International pour l'Exploration de la Mer, Proces et Verbaux*, **112**, 77–94.

TAYLOR A. H. and J. A. STEPHENS (1980) Seasonal and year-to-year variations in surface salinity at the nine North Atlantic ocean weather stations. *Oceanologica Acta*, **3**, 421–430.

VAN BENNEKOM A. J. and S. B. TIJSSEN (1978) Nutrients on and off the Guyana shelf related to upwelling and Amazon outflow. In: *CICAR II. Progress in marine research in the Caribbean and adjacent regions*, H. B. STEWART JR, editor, *FAO Fisheries Report*, **200**, suppl., 233–253.

YOO J. M. and J. A. CARTON (1990) Annual and interannual variation of the freshwater budget in the tropical Atlantic Ocean and the Caribbean Sea. *Journal of Physical Oceanography*, **20**, 831–845.

APPENDIX

For using the kriging method, it is assumed that the physical phenomena studied have a regionalized pattern, and that a stable structure exists on which random anomalies are superimposed (MATHERON, 1971).

In order to model this structure, an experimental variogram is first drawn (more exactly a half variogram). This is evaluated in grouping measurement pairs made during different years by class of distance defined with a degree mesh. The studied structure is assumed isotropic so that direction is not taken into account. The density of the data varies with the location, and consequently the data number has been limited at a maximum of three inside a mesh for any month; a random drawing is done when there are more than three observations. Thus, the SSS value in each mesh of the grid is estimated from the closest point by considering 4 by 4 of the grid points of the increasing crowns, until a minimum number of previously fixed points is reached. If there are more, all the points inside the crown however, are saved. The variogram does not usually pass through the origin because of a "nugget effect", which in this present case is due to measurement errors and to the year-to-year and month-to-month variability, since the time of the measurement is not taken in account. The areas where low salinities appear (outflows of large rivers) with a strong SSS variability will increase the value of the "nugget".

The noise affecting the measurements is greatest when the values are weakest (spatial variability induced by local rainfall, spreading of river outflow, etc.). As suggested by GOHIN and LANGLOIS (1991), it would be preferable to determine separate variograms for those areas with strong variability and for areas with smaller variability (outside 10°N for example). The increase of the variance with the small salinity values has led us to exclude the small number of SSS less than 25.0 p.s.u. The adjustment of the experimental variogram is made by a theoretical model with a preference for the middle distance (until about 10°) and neglecting the random variations close to the origin. The errors due to the kriging method are homogeneous in the whole studied area, with values between 0.65 and 0.70 p.s.u., except south of 5°S where the sampling is scarce and where values reach 0.80 p.s.u.

After estimating the experimental variogram, doubtful data are detected and eliminated; they may be due to faulty samples but also data collected at time or in area where the local variability is particularly strong: a SSS different by 3 or 4 p.s.u. from the surrounding values is not compatible with the climatology and also may disturb strongly the spatial structure of the field, if occurring in less well sampled regions. Practically all observations are again estimated by considering the close points belonging to different years and selected by the previous procedure. The observation is discarded if the deviation between the estimated and observed values is more than p times the theoretical RMS of the kriging. This eliminates less than 0.5% of the observations. The variogram is again evaluated. The estimation of the salinity at every node of the grid is then done from the closest points belonging all to different years. The minimum of such closest points being fixed at six; if there are less than 6 points located in an 8° distance from the point to estimate, the kriging procedure is cancelled. Consequently, in the area with insufficient sampling, the estimation was not possible at some node of the grid.

One of the advantages of the kriging method relative to the other method of objective analysis, is to allow the calculation of the variance of the estimations, variances depending only on the location of the experimental points in the considered field and to the structure of the studied phenomena (modeled by the variogram). Consequently, the variance of the estimation depends on the model of the variogram (GOHIN and LANGLOIS, 1991). The kriging method also has been used for objective mapping of marine variables such as primary productivity (HERZFELD, 1992).